INVESTIGATION OF SECOND-MOMENT-CLOSURE DEFECTS IN SEPARATED BOUNDARY LAYER BY REFERENCE TO HIGHLY-RESOLVED LES DATA

Yacine Bentaleb, Sylvain Lardeau and Michael A. Leschziner
Department of Aeronautics, Imperial College London
Prince Consort Rd, London SW7 2AZ
y.bentaleb@imperial.ac.uk s.lardeau@imperial.ac.uk
mike.leschziner@imperial.ac.uk

ABSTRACT

A second-moment-closure model, selected following a preliminary study of several models of the same class, is subjected to extensive *a-priori* analysis in a flow separating from a curved surface, leading to a newly proposed corrections aimed specifically at the separated shear layer. The analysis includes a separate examination of the dissipation-rate equation, the dissipation anisotropy and the pressure-strain correlation, with the aim of clarifying the validity and effectiveness of various components therein. This is done by reference to highly-resolved LES data recently generated by Lardeau et al. (2011) for a canonical turbulent boundary layer separating from a curved ramp, with results including a complete set of second-moment budgets. The nature of the *a-priori* tests is described, and the outcome discussed.

INTRODUCTION

Second-moment-closure (SMC) models are generally expected to give superior predictive capabilities in complex flows containing a variety of strain types and subjected to body forces. However, many validation studies (e.g. Wang et al., 2004) demonstrate that this expectation has only been fulfilled to a limited extent, and this has discouraged the adoption of complex SMC models in industrial CFD practice. While SMC models often perform well when simple shear is combined with one other type of "complex" strain (e.g. curvature), SMC models often give results that are no better, or even worse, than carefully calibrated eddy-viscosity models when several types of strain interact in a geometrically complex setting.

A particularly problematic group of flows comprises those in which separation occurs from gently curved surfaces – the prevalent type in engineering practice. Relative to flows separating from a sharp corner, these are characterised by a significant streamwise stretch over which the flow is intermittently separated and attached. This process results in an especially high level of unsteadiness in the separated shear layer downstream of the time-averaged separation location and also within the recirculation region below the shear layer. One statistical manifestation of this unsteady separation is an extremely high level of turbulence energy and stress in the separated shear layer, reflecting levels of turbulence-energy production that exceed the dissipation rate by factors of up to 4. Others are the formation of a thin recirculation zone, with an extremely pointed wedge of reverse-flow layer downstream of separation, and early reattachment at a very shallow angle.

While there is a significant variability among models in terms of the details of the solutions they yield, a recurring defect is that most predict insufficient levels of turbulence activity in the separated shear layer and thus, generally, a serious delay in reattachment and excessive recirculation, shortcomings that reflect an inability of the models to account for the dynamics of the separation process, made worse by the tendency of the models to depress the turbulent stresses in the shear layer bordering the recirculation zone because of the effects of (stabilizing) curvature on the turbulent stresses. For second-moment models to become an attractive modelling category in practice, especially in view of their complexity, their ability to predict separation and recirculation must be improved significantly. This has to be done, preferentially, with closure forms that are not too elaborate, because numerical intractability goes hand-in-hand with mathematical complexity and the increased non-linearity involved.

The present paper reports a study of a particular SMC model (Jakirlić and Hanjalić, 1995), selected based upon preliminary computations with several models to identify the best candidate for further study and, ultimately, for improvement directed specifically at separation from curved surfaces. The emphasis of the study is on *a-priori* examinations of the validity of specific model components and terms in the separated shear layer, and on related improvements. The key to such efforts is the availability of accurate and detailed reference data for pertinent geometries. The one preferred herein was generated very recently by Lardeau et al. (2011) with highly-resolved (near-DNS) LES for a turbulent boundary layer separating from a curved ramp. This case is geometrically simple, yet physically complex, readily controlled in respect of mesh quality and supported by accurate unsteady inlet conditions. Data available for comparisons include a complete set of second-moment budgets and various fields for length-scales and ratio of statistical quantities.

DESCRIPTION OF THE FLOW

The geometry under consideration is shown in Fig. 1. The ramp is an enlargement of that used originally by Song and Eaton (2004). At $x/H = -7.36$, a (close to) canonical zero-pressure-gradient boundary layer, at momentum-thickness Reynolds number $Re_\theta = 1193$, $Re = 13700$ (based on the step height H and inlet free-stream velocity U_{in}) and boundary-layer thickness $\delta_{99} = 0.83H$, was prescribed by injecting up to $150,000$ instantaneous realisations, covering $1120H/U_{in}$, and obtained from a separate highly-resolved LES precursor simulation, with statistics matching published DNS data. The actual LES, being close to a DNS, was performed over a spanwise domain of $3.7H$ with a mesh of 24 million nodes, using a second-order collocated finite-volume code. The ratio of Kolmogorov to cell dimension was below 10, and the SGS viscosity, obtained with a mixed-time-scale model, was below 0.2 of the fluid viscosity. More details about the LES will be reported in a separate paper (Lardeau et al., 2011) currently in preparation.

A few sample results are presented (Fig. 2) to illustrate some salient features of the separated flow. Figure 2a shows the time-averaged stream-function field, depicting the recirculation region. An extremely thin and elongated separation zone and subsequent shallow reattachment are observed. The zero-streamwise-velocity locus (dashed-dot line), essentially bisecting the recirculation zone, is seen to be close to the wall over a substantial proportion of the reverse-flow region downstream of the separation point. Despite this proximity, the early stage of separation is marked by a rapid increase in turbulence energy and shear stress, primarily driven by very high production, provoking large departures from equilibrium conditions. The turbulence-production-to-dissipation ratio, shown in Fig 2b, increases drastically following separation, reaching a maximum value of 3.3 at around $x/H \approx 1$. The strong rise in turbulence intensity is dominated by the streamwise contribution, resulting in very high levels of anisotropy, with only a gradual redistribution to other components. This is reflected by low levels of Lumley's "flatness parameter", $A = 1 - 1.125(A_2 - A_3)$, formed from the second and third stress-anisotropy invariants, with $A = 1$ representing isotropy. The contour plot in Fig. 2c shows that this parameter is especially low (of order 0.1) in an elongated thin layer near the separation point, gradually increasing as the shear layer evolves. However, the anisotropy level remains substantial in central portions of the free shear region.

SELECTION OF SMC MODELS

A generic representation of the SMC models considered herein is as follows:

$$\frac{D\overline{u_i u_j}}{Dt} = P_{ij} - \varepsilon_{ij} + T_{ij} + \Phi_{ij} + D_{ij} \qquad (1)$$

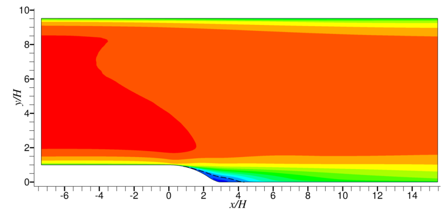

Figure 1: Geometry of the flow configuration, including the streamwise mean-velocity field.

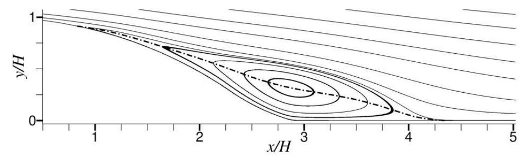

(a) Streamline contours of the time-averaged flow field. The dashed-dot line represents the zero-streamwise-velocity locus. Separation: $x/H = 0.83$; reattachment: $x/H = 4.36$.

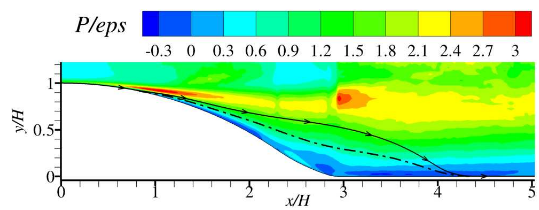

(b) Turbulence-production-to-dissipation ratio

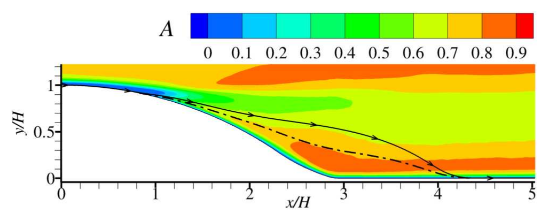

(c) Flatness parameter contours.

Figure 2: Sample results from LES computation.

where P_{ij}, ε_{ij}, T_{ij}, Φ_{ij} and D_{ij} represent, respectively, production, dissipation, turbulent transport, pressure-strain correlation and diffusion, the last combining pressure and viscous contributions.

The starting point of the present work is the computation of the flow described above with four existing low-Reynolds-number SMC models. The choice of models was guided by two main considerations: popularity of use and relative simplicity; the latter being of importance to an industrial uptake, thus dictating the omission of complex models using high-order pressure-velocity-interaction approximations. Three closures were included in the preliminary selection stage: (i) the Shima (1998) model; (ii) the Jakirlić and Hanjalić (1995) model (hereafter designated JH) and (iii) a low-Reynolds extension (Chen et al., 2000) of the Speziale et al. (1991) model, the last of which using a relatively simple quadratic formulation (hereafter designated SSG+C). Model solutions were first compared with the reference LES data, but only a small

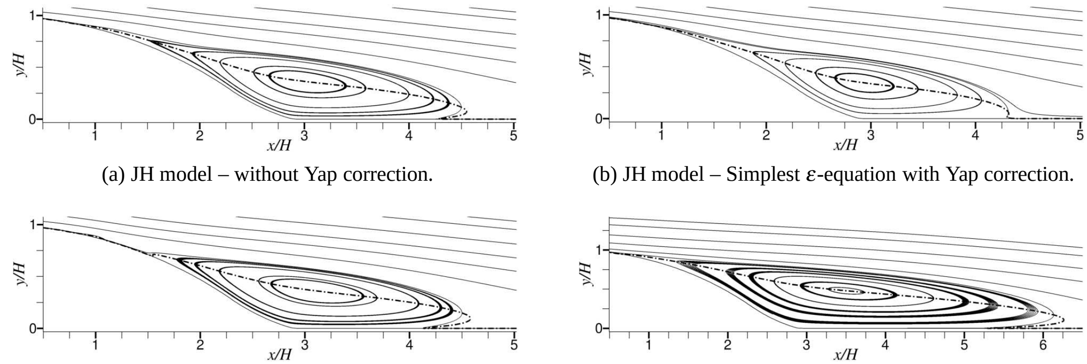

(a) JH model – without Yap correction.

(b) JH model – Simplest ε-equation with Yap correction.

(c) SSG+Chen (1991/2000) model.

(d) Shima (1998) model.

Figure 3: Streamline contours, including the zero-streamwise-velocity locus (dashed-dot line) – Full computations.

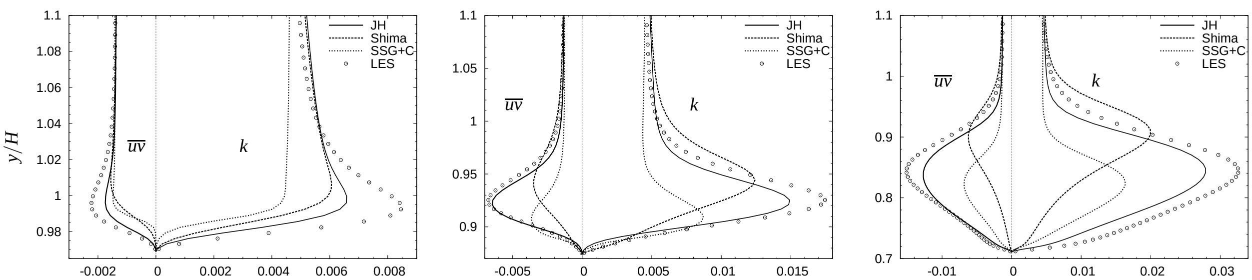

(a) $x/H = 0.5$

(b) $x/H = 1.0$

(c) $x/H = 1.5$

Figure 4: Turbulence energy and shear-stress profiles normalized by U_{in}^2 – Full computations.

selection of this comparison can be included herein. Figure 3 shows model-predicted stream-function fields, the LES reference solution being given in Fig. 2a. As is commonly observed in separated flows, the models yield excessively large recirculation zones, and feature, in addition, an abnormal reattachment behaviour, wherein the streamwise velocity changes sign twice in the wall-normal direction. A widespread practice, aimed to suppress (or reduce) the latter behaviour, is the use of a source term in the dissipation-rate equation, often referred to the "Yap correction" (although this includes several related variants). An illustration of its phenomenologically "beneficial" effect at reattachment is given in Fig. 3b in comparison with Fig. 3a, but the effect will be shown latter, upon closer examination, to be incompatible with the underlying rationale of the correction. As confirmed by the turbulence energy and shear stress profiles included in figure 4, of the models considered, the JH form performs best, and this was thus singled out for detailed *a-priori* studies.

The selected models differ mainly in respect of the approximations for the pressure-strain process Φ_{ij} and dissipation tensor ε_{ij} they incorporate. Both are highly influential. While the common argument used in relation to most models is that the anisotropic component of ε_{ij} can be absorbed into the model for Φ_{ij}, the JH proposal for ε_{ij} includes an explicit approximation targeting primarily the near-wall region, but also affecting wall-remote shear layers. Moreover, the closure involves the dissipation-rate invariant E, analogous to the flatness parameter A, in addition to the latter, to represent the wall-blockage effects. The former is used both in the "slow" fragment of Φ_{ij}, and in the dissipation ε_{ij} model itself. It is noted that each SMC model may be used with one of several variants of the dissipation-rate equation, differences being rooted, for example, in the inclusion or omission of auxiliary source/sink terms. The following section examines, through *a-priori* studies, the effectiveness and relevance of the above specific model fragments, focusing on the separated shear layer.

A-PRIORI STUDIES

A model modification introduced ahead of undertaking the *a-priori* studies, was to replace the dissipation ("flatness") invariant E by use of A. The primary motivation is two-fold. First, this allows separate (decoupled) investigations of the modelled dissipation tensor and the pressure-strain correlation to be performed. Second (and linked to the former), the LES does not allow reliable data for E to be obtained, and this makes it very difficult to pursue targeted model improvements based on the *a-priori* analysis in which E is included. A third argument is that preliminary studies had shown the dissipation components to be well approximated by the algebraic expression $\varepsilon_{ij} = \varepsilon \overline{u_i u_j}/k$, at least in the separated shear layer, which is of primary interest in the present study. The replacement of E by A^n (with $n = 0$, 0.5, and 1), and even by $E = 0$, has been found to have very minor consequences to the mean-flow solutions.

The *a-priori* analysis of models fragments is presented below, starting with the dissipation equation, and intended to address the relevance of the non-standard source terms which are part of the JH model. An improved proposal is also suggested. Then, the dissipation tensor and pressure-strain approximations are examined, with emphasis placed on assessing the above replacement of E by A^n.

Dissipation-rate equation

With the non-standard source terms excluded, the dissipation-rate equation is:

$$\frac{D\varepsilon}{Dt} = \frac{\partial}{\partial x_k}\left[\left(\nu\delta_{kl} + C_\varepsilon \frac{k}{\varepsilon}\overline{u_k u_l}\right)\frac{\partial \varepsilon}{\partial x_l}\right] + C_{\varepsilon_1}\frac{\varepsilon}{k}\,\overline{u_i u_j}\,\frac{\partial U_i}{\partial x_j} - C_{\varepsilon_2}\frac{\varepsilon\tilde{\varepsilon}}{k} \quad (2)$$

where the coefficients take the standard values ($C_\varepsilon = 0.18$, $C_{\varepsilon_1} = 1.44$ and $C_{\varepsilon_2} = 1.92$). One extra source term included in the JH model is a Yap-like correction that is sensitised to the wall-normal derivative of the integral length scale. Here, a simpler variant is examined, much closer to the original form proposed by Yap (1987):

$$S_l = \max\left\{\left(\frac{l}{l_e}-1\right)\left(\frac{l}{l_e}\right)^2;0\right\}\frac{\tilde{\varepsilon}\varepsilon}{k}A \quad (3)$$

where $l = k^{3/2}/\varepsilon$, $l_e \equiv C_\mu^{-0.75}\kappa y_n \sim 2.5 y_n$ is the equilibrium length-scale and A the flatness parameter.

The *a-priori* test consists on inserting the LES-derived mean velocity and Reynolds stresses into Eq. 2, and solving it in isolation (*i.e.* with all other quantities frozen). Predicted dissipation profiles returned by this test, at various vertical streamwise locations ($x/H = 0$, 0.5, 1, 1.5, 3 and 4), are shown in Fig. 5 by reference to LES data. In this figure, *simple* identifies Eq. 2, while *original* identifies the JH-model form, excluding the Yap-like term. The best result is obtained with the simple form in the separated shear layer. The addition of the Yap correction results in a collapse of the dissipation in the separated shear layer, and is therefore counterproductive. In the full computation, with all model equations active, the Yap correction is also observed to be detrimental to accuracy, as emerges from Fig. 6. The term in Eq. 3 tends to decrease the length scale relative to its equilibrium value, l/l_e, which is already low, however, without this correction in the separated region, especially near the reattachment point ($x/H = 4.36$). To summarize without further details, it has been found that the extra source/sink terms in the JH form of the dissipation-rate equation, including the Yap correction, either offer no benefit or are counter-productive.

To steer the dissipation rate towards the reference data, an alternative practice is investigated here. Noting the large departure from turbulence-energy equilibrium in the separated shear layer (see Fig. 7), and taking advantage of the stress-anisotropy variations, we suggest to modify the destruction term of the ε–equation. Specifically, the following proposal is considered and examined in an *a-priori* sense:

$$C'_{\varepsilon_2} = C_{\varepsilon_2}\left(1 + f(A,A_2)\left|\frac{P_k}{\varepsilon}-1\right|\right) \quad (4)$$

where f is a function of the stress invariants A and/or A_2. Figure 8 shows the results for different functional forms: $f = A_2/8$, $f = (1-A)/8$ and a constant value $f = 0.2$. Improvements are observed at the early stages of separation (e.g. at $x/h = 1.5$), but is further room for an optimization that yields better agreement throughout the shear layer.

Dissipation-rate tensor

The second model component examined here is the dissipation anisotropy. The tensorial model used in Jakirlić and Hanjalić (1995) is as follows:

$$\varepsilon_{ij} = f_s\varepsilon^*_{ij} + (1-f_s)\frac{2}{3}\delta_{ij}\varepsilon, \qquad f_s = 1-\sqrt{A}E^2 \quad (5)$$

$$\varepsilon^*_{ij} = \frac{\varepsilon}{k}\frac{\overline{u_i u_j} + (\overline{u_i u_k}n_j n_k + \overline{u_j u_k}n_i n_k + \overline{u_k u_l}n_k n_l n_i n_j)f_d}{1+\frac{3}{2}\frac{\overline{u_p u_q}}{k}n_p n_q f_d} \quad (6)$$

where $\boldsymbol{n}$ is the unit normal to the wall, $Re_t = k^2/(\varepsilon\nu)$ the turbulence Reynolds number, $\frac{2}{3}\varepsilon\delta_{ij}$ the isotropic dissipation, ε^*_{ij} stands for the dissipation tensor in the near-wall region, f_s being the blending function of the last two quantities, and $f_d = (1+0.1Re_t)^{-1}$.

The replacement of the parameter E in Eq. 5, discussed earlier, is considered here. In the present *a-priori* test, LES-derived fields for ε and $\overline{u_i u_j}$ are inserted into Eq. 6 to derive ε^*_{ij}. Then f_s and ε_{ij} are computed. In other words, no equation is solved, other than (5) and (6). The normalized dissipation components, $\tilde{\varepsilon}_{ij} = \varepsilon_{ij}/\frac{2}{3}\varepsilon$, are reported in Fig. 9. The use of a blending function (and consequently the E-paramater therein) turns out to be ineffective. In fact, both the anisotropic part of the dissipation-tensor model, ε^*_{ij} (corresponding to $E = 0$), and the Rotta model, $\varepsilon\overline{u_i u_j}/k$, provide good approximations prior to separation and in the separated shear layer, by comparison to the reference data.

Pressure-strain correlation

The final test reported in this paper concerns the pressure-strain approximation. This test entails the insertion of the LES data into the related JH modelled term:

$$\Phi_{ij} = -C_1\varepsilon a_{ij} - C_2\left(P_{ij} - \frac{2}{3}P_k\delta_{ij}\right) + \Phi^w_{ij} \quad (7)$$

$$C_1 = C + \sqrt{A}E^2, \quad C_2 = 0.8A^{1/2}, \quad C = f(A,A_2,Re_t) \quad (8)$$

where the wall-reflection redistribution term, Φ^w_{ij}, is not given here. It does not contain E, in any event. The pressure-strain correlation is highly influential, and its approximation is the principal source of differences among SMC models, especially in the vicinity of separation. A misrepresentation of the energy redistribution process in highly anisotropic sheared regions necessarily leads to wrong productions. In the case

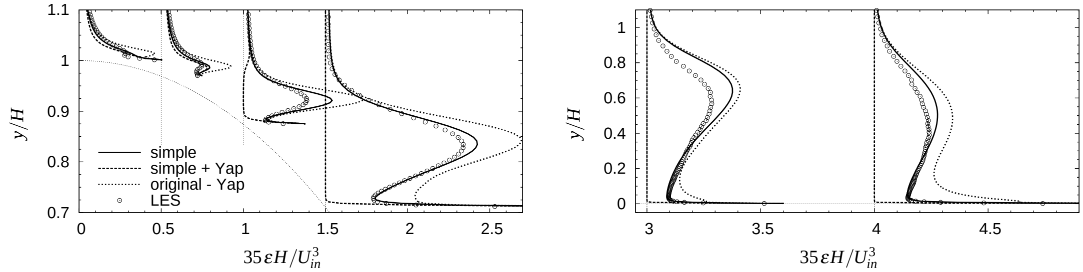

Figure 5: Dissipation-rate profiles at various streamwise locations – A-priori tests.

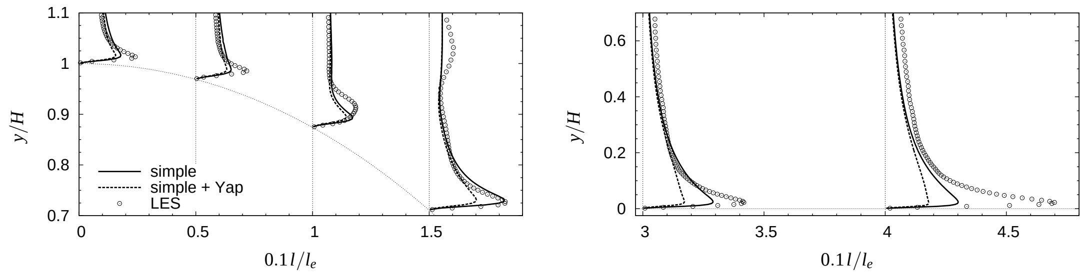

Figure 6: Length-scale ratio l/l_e at various streamwise locations – Full computations.

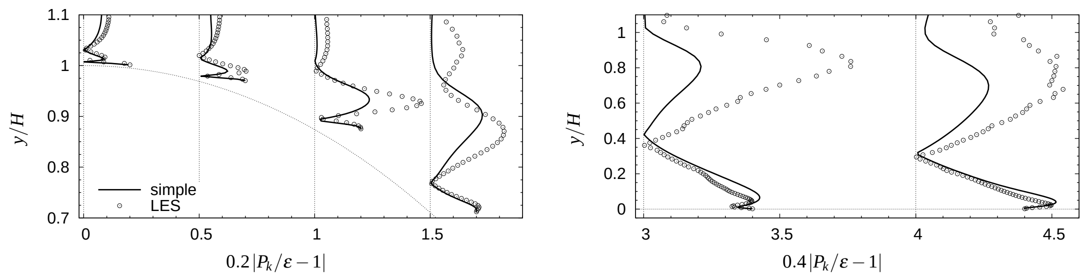

Figure 7: Departure from turbulence-energy equilibrium. Profiles at various streamwise locations – Full computations.

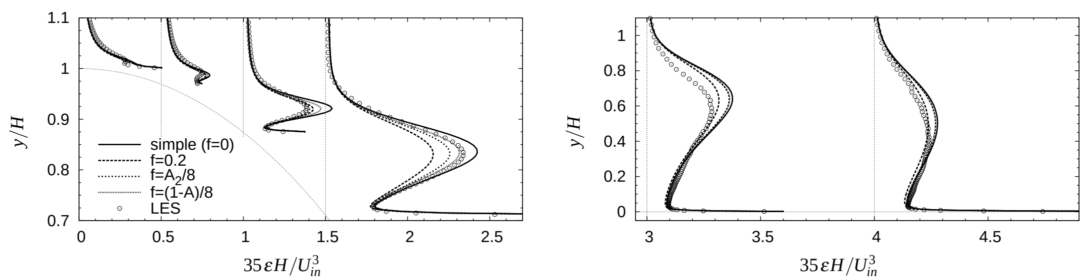

Figure 8: Dissipation-rate profiles at various streamwise locations – A-priori tests of the proposals.

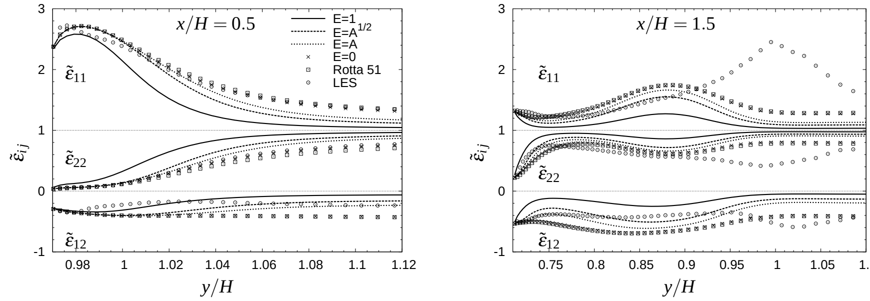

Figure 9: Normalized dissipation components $\tilde{\varepsilon}_{ij} = \varepsilon_{ij}/\frac{2}{3}\varepsilon$ at two streamwise locations – A-priori study.

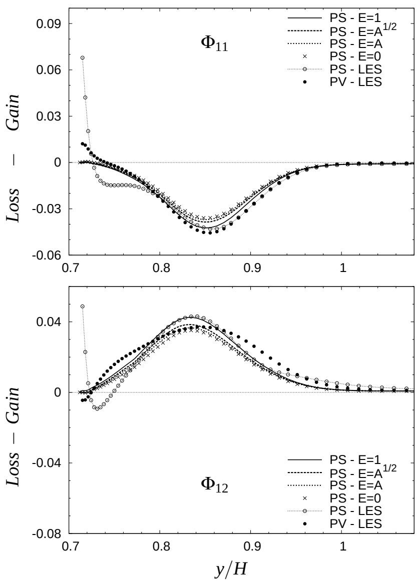

Figure 10: Pressure-strain contributions Φ_{11} and Φ_{12} (PS) at $x/H = 1.5$ – A-priori study. LES-derived pressure-velocity interaction (PV) is also included.

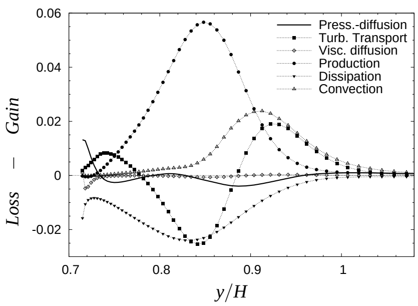

Figure 11: k-budget at $x/h = 1.5$ – from LES data.

of separation from curved walls, the main defects observed are depressed turbulence energy and shear stress in the initial stretch of the separated shear layer. A particular position, $x/H = 1.5$, where the maximum shear-stress and turbulence productions occur in the separated shear layer, is selected to illustrate the nature and outcome of the *a-priori* study. Figure 10 shows the pressure-strain contribution in the $\overline{uu}$ and $\overline{uv}$ budgets in that particular location. First, it is recognised that the sensitivity of the model to the replacement of E is marginal. Second, the LES-derived pressure-velocity correlation (as contrasted with the pressure-strain part alone), also included in the figure, is close to the modelled pressure-strain fragment in the separated shear layer. Specifically in relation to the last observation, Fig. 11 shows, for the same location, the LES-derived turbulence-energy budget. The pressure-diffusion component, representing the departure of the pressure-velocity correlation from the contracted (zero-valued) pressure-strain term. This departure is low compared to the prime components (production, turbulent transport and dissipation rate), except near the wall, and this suggests the zero-divergence constraint applied to the modelling of the pressure-strain process is of little importance. Thus, in the present context of predicting separated flow, the decomposition of the pressure-velocity interaction into pressure-strain and pressure-diffusion, the latter assumed to supplement turbulence diffusion, appears to be of little relevance. The fact is that the "pressure-strain model" is a much better approximation of the complete pressure-velocity interaction than it is of the true pressure-strain part. The implication is that pressure-diffusion need not be modelled separately.

CONCLUSIONS

The *a-priori* analysis of the particular model selected has highlighted the redundancy, or even detrimental effects, of several auxiliary source/sink terms in the dissipation-rate equation, and the overly elaborate nature of the tensorial approximation of the anisotropic dissipation-rate components in the separated shear layer. To achieve a better representation of dissipation, a specific proposal has been made, but its effectiveness throughout the flow has yet to be verified by full computations. Finally, it has been shown that separate modelling of the pressure-strain correlation and pressure-diffusion is of little relevance. The pressure-strain model is, in effect, a fair approximation of the pressure-velocity interaction as a whole, despite the former being subject to a zero-divergence constraint.

ACKNOWLEDGMENT

This work was funded by the EC project ATAAC, 7^{th} Framework Prog. (No. ACP8–GA–2009-233710-ATAAC).

REFERENCES

H.C. Chen, Y.J. Yang, and J.C. Han. Computation of heat transfert in rotating two-pass square channels by a second-moment closure model. *Int. J. Heat Mass Transfer*, 43: 1603–1616, 2000.

S. Jakirlić and K. Hanjalić. A second-moment closure for non-equilibrium and high- and low-Re-number flows. *Proc. 10th Symp. on Turbulent Shear Flows, Pennsylvania State University*, 1995.

S. Lardeau, Y. Bentaleb, and M.A. Leschziner. Large Eddy Simulation of turbulent boundary-layer separation from a rounded step. *Private communication*, 2011.

N. Shima. Low-Reynolds-number second-moment closure without wall-reflection redistribution terms. *Int. J. Heat Fluid Flow*, 19(5):549–555, 1998.

S. Song and J.K. Eaton. Reynolds number effects on a turbulent boundary layer with separation, reattachment and recovery. *Experiments in Fluids*, 36(2):246–258, 2004.

C.G. Speziale, S. Sarkar, and T.B. Gatski. Modelling the pressure-strain correlation of turbulence: an invariant dynamical systems approach. *J. Fluid Mech.*, 227:245–272, 1991.

C. Wang, Y.J. Jang, and M.A. Leschziner. Modelling two- and three-dimensional separation from curved surfaces with anisotropy-resolving turbulence closures. *Int. J. Heat Fluid Flow*, 25(3):499–512, 2004.

C.R. Yap. *Turbulent heat and momentum transfer in recirculating and impinging flow*. PhD thesis, Faculty of Technology, University of Manchester, 1987.